ELSEVIER

Journal of Molecular Catalysis A: Chemical 113 (1996) 427–444

JOURNAL OF MOLECULAR CATALYSIS A: CHEMICAL

Oxide-supported triruthenium ketenylidene clusters and their catalytic properties

Feng-Shou Xiao [a,*], Masaru Ichikawa [b]

[a] *Department of Chemistry, Jilin University, Changchun 130023, China*
[b] *Catalysis Research Center, Hokkaido University, Sapporo 060, Japan*

Received 1 December 1995; accepted 29 April 1996

Abstract

A triruthenium ketenylidene cluster, $[PPN]_2[Ru_3(CO)_6(\mu\text{-}CO)_3(\mu_3\text{-}CCO)]$ (**1**), as a possible precursor for production of higher oxygenates, was deposited on MgO, SiO_2 and SiO_2–Al_2O_3, and the nature of surface species supported on these oxides was characterized by IR and Raman spectroscopy along with their catalytic performance in CO isotopic exchange, alkylation, and hydroformylation. When MgO was dehydrated below 573 K, the sample spectrum of the triruthenium ketenylidene cluster on the MgO support exhibited characteristic bands of $[Ru_3(CO)_6(\mu\text{-}CO)_3(\mu_3\text{-}CCO)]^{2-}$. A new surface species assigned to $[HRu_3(CO)_9(\mu_3\text{-}CCO)]^-$ (**2**) was characterized by new IR bands at 2068, 2030, and 1999 cm^{-1}, as the MgO was dehydrated at 673 K. On SiO_2 and SiO_2–Al_2O_3, IR investigation suggested that the stoichiometric protonation of $[Ru_3(CO)_6(\mu\text{-}CO)_3(\mu_3\text{-}CCO)]^{2-}$ (**1**) with surface hydroxyl groups such as Si–OH and Si(OH)Al occurred, giving rise to $[HRu_3(CO)_9(\mu_3\text{-}CCO)]^-\{SiO^-\}$ (**2**) and $H_2Ru_3(CO)_9(\mu_3\text{-}CCO)2\{Si(O^-)Al\}$ (**3**), respectively. The above mentioned species were demonstrated by the extraction from surface species by IR and NMR investigation. The Raman spectra of MgO and SiO_2 supported triruthenium clusters showed bands assigned to Ru–Ru and Ru_3–C stretching modes. In the reactions of CO isotopic exchange, alkylation and hydroformylation, these oxides-supported triruthenium ketenylidene species showed quite different activities. $H_2Ru_3(CO)_9(\mu_3\text{-}CCO)2\{Si(O^-)Al\}$ (**3**) was active for CO isotopic exchange reaction, while $[Ru_3(CO)_6(\mu\text{-}CO)_3(\mu_3\text{-}CCO)]^{2-}\{MgO\}$ (**1**) was active with CH_3I at room temperature in alkylation reaction. In hydroformylation of ethylene, MgO-supported triruthenium ketenylidene species showed high activity and selectivity for formation of oxygenates, while the SiO_2–Al_2O_3-supported triruthenium ketenylidene cluster exhibited a high activity for the formation of ethane. These results have demonstrated that the support effect is obvious for the formation of various triruthenium ketenylidene species on oxides. Additionally, the preparation of these triruthenium ketenylidene clusters on oxides by *surface-mediated organometallic synthesis* showed a very high yield and a relatively simple procedure as compared with those by *solution synthesis*.

Keywords: Cluster; Ketenylidene; Oxide; Extraction; CO isotopic exchange; Alkylation; Hydroformylation

1. Introduction

A better understanding of the effect of the support material on catalytic behavior is important and may provide guidance in choosing or designing a better catalyst for catalytic reactions. It has been reported that the nature of oxide supports markedly influenced the production distribution in CO hydrogenation on supported metal catalysts [1]. Rh catalysts prepared from $[Rh_4(CO)_{12}]$ on TiO_2, ZrO_2, La_2O_3, and

* Corresponding author. Fax: +86-431-8923907. E-mail: fsxiao@mail.jlv.edu.cn

PII S1381-1169(96)00183-5

Nb_2O_3, gave ethanol and acetaldehyde to considerable amounts. Methanol was produced over the Rh clusters supported on ZnO, MgO, and CaO supports, while methane was a major product on SiO_2–Al_2O_3 [2]. It is a quite challenging subject to understand the chemical origins of supporting oxides managing the product distribution in catalytic reactions on supported transition metal catalysts.

Metal clusters are very useful precursors for the design of active centers in heterogeneous catalysis, because they have small sizes and definite compositions of metal frameworks [3–8]. Also, metal clusters supported on oxide supports offered opportunities to understand the elementary steps of heterogeneous catalytic reactions and the metal-support interaction [4–8]. A number of metal carbonyl clusters on oxide supports have been widely used as the catalytic precursors in CO-based reactions such as CO hydrogenation, olefin hydroformylation, and water–gas shift reaction, since these clusters are possible intermediates in these catalytic reactions.

Doubly negative triruthenium ketenylidene clusters $[PPN]_2[Ru_3(CO)_9(\mu_3\text{-}CCO)]$ (**1**) protonated sequentially on the metal framework to yield mononegative ketenylidene $[PPN][HRu_3(CO)_9(\mu_3\text{-}CCO)]^-$ (**2**) and neutral ketenylidene $H_2Ru_3(CO)_9(\mu_3\text{-}CCO)$ (**3**) in the solution [9–13]. These ketenylidene clusters were possible intermediates for the formation of C_2-oxygenates in CO hydrogenation over supported metal catalysts, which are easily attacked by the chemical groups. The transformation of the ketenylidene clusters by the reaction with nucleophiles and electrophiles has been extensively investigated. The triruthenium ketenylidene clusters may be good precursors for investigation of support effects for the formation of surface species and the catalytic properties.

In this paper, our goals were to study the support effect by using triruthenium ketenylidene clusters supported on oxides having different acid–base properties, to characterize the adsorption of the triruthenium ketenylidene cluster supported on oxides, and to investigate their catalytic properties. Here we report (1) the infrared spectra of surface species on various oxides and of the solution extracted from these surface species, (2) Raman evidence of these surface species, and (3) catalytic activities in ^{13}CO exchange reaction, alkylation of CH_3I and CH_3Li, and ethylene hydroformylation.

2. Experimental

2.1. Materials

All syntheses and sample transfers were conducted with exclusion of air and moisture on a double-manifold Schlenk line and in an N_2-filled Braun glove box. N_2 and H_2 with purity of 99.999% (Takachiho) passed through beds of Cu_2O and 4A zeolite to remove traces of O_2 and moisture. CO and ^{13}CO (isotopic purity 99.3%) used in isotopic exchange reaction were purchased from MSD Isotopes. The agents of alkylation reaction such as CH_3I (purity 99.7%) and CH_3Li (purity 99.5%) were supplied from Sigama Chemical. The CO used in ethylene hydroformylation was passed through a bed of activated alumina heated to a temperature exceeding 200°C to remove traces of iron carbonyl contaminants and through a bed of 4A zeolite to remove moisture. Ethylene was purchased from Takachiho without further purification. Solvents were distilled from the appropriate drying agents [14], and followed by deoxygenation in flowing dry N_2 prior to use.

Porous MgO (MX-65-1 powder, MCB reagents, surface area approximately 70 m^2/g), Aerosil 300 (Nippon Aerosil), and silica–alumina (Nippon Aerosil) were used as supports of MgO, SiO_2, and SiO_2–Al_2O_3, respectively. The MgO was dehydrated at various temperatures such as 473, 573, and 673 K, which were referred to as MgO_{473}, MgO_{573}, and MgO_{673}, respectively. The Na^+ ions presented in the SiO_2–Al_2O_3 support were exchanged with H^+ by treatment of an aqueous solution of NH_4Cl

(0.1 N) at 368 K. After removing water, the SiO_2–Al_2O_3 support was calcinated in air at 823 K for 2 h. This exchange/calcination was repeated three time to complete the ion-exchange, giving the H-type of SiO_2–Al_2O_3.

2.2. IR spectra of the Ru ketenylidene cluster on oxides

Powders of the oxides were pressed into disks (30–35 mg, diameter 20 mm), and mounted in an IR cell with CaF_2 or KBr windows. The disks were evacuated at the required temperature for 2 h, and cooled down to room temperature. After 2 mg of **1** was dissolved in 0.2 ml of CH_2Cl_2 under 1 atm of N_2, the solution was dropped onto the disks through the injection part of the cell without air contamination, then the CH_2Cl_2 was removed under vacuum at room temperature. The Ru loading is about 1 wt%. Infrared spectra were recorded in transmission mode on a double-beam Fourier-transform infrared spectrometer (Shimadzu FTIR-4100) with a spectral resolution of 2 cm^{-1} and a precision of 1 cm^{-1}.

2.3. Preparation of the MgO supported Ru ketenylidene cluster

The MgO-supported triruthenium ketenylidene sample was prepared by adsorption of **1** on MgO. The **1** precursor dissolved with CH_2Cl_2, was slurried with MgO powder dehydrated at the required temperature. The slurry was stirred for 30 min, followed by solvent removal by evacuation for 4 h. The Ru loading is controlled by the change in precursor amount.

2.4. Preparation of the SiO_2 supported Ru ketenylidene cluster

The SiO_2-supported triruthenium ketenylidene sample was prepared by adsorption of **1** precursor with SiO_2 support dehydrated at 573 K for 2 h in CH_2Cl_2 solvent. The slurry was stirred for 30 min, followed by solvent removal by evacuation for 4 h.

2.5. Preparation of the SiO_2–Al_2O_3 supported Ru ketenylidene cluster

The SiO_2–Al_2O_3-supported triruthenium ketenylidene sample was prepared by adsorption of **1** precursor with SiO_2–Al_2O_3 support dehydrated at 573 K for 2 h in CH_2Cl_2 solvent. The slurry was stirred for 30 min, followed by solvent removal by evacuation for 4 h.

2.6. Preparation of 2 and 3

The preparation of **2** and **3** followed published literature [10].

2.7. IR spectra of extracted solutions

Extraction of triruthenium ketenylidene clusters from the surface species was performed by mixing solid samples with [PPN][Cl] [PPN = bis(triphenylphosphine) nitrogen(+1)] in CH_2Cl_2, and followed by adding solvent. The mixture was stirred for about 10 min, and the resultant color of the solution and the loss of color of the powder (it became white) indicated when the extraction was complete. The solution was transferred with an airtight syringe to a sealed infrared cell, and the spectroscopic characterization was completed within a few minutes. Infrared spectra were recorded with a Bruker IFS66V spectrometer with a spectral resolution of 2 cm^{-1} and a precision of 1 cm^{-1}. NMR ^{13}C spectra were measured with a Varian XL-400 spectrometer, and the reference of the ^{13}C spectra was external Me_4Si.

2.8. Raman spectra of oxides-supported Ru ketenylidene clusters

Raman spectra were obtained by krypton laser excitation (6471 or 6764 Å) filtered by a premonochromator to remove the laser plasma line. A standard Spex solid sample rotator was used to prevent thermal or photochemical decomposition, and the Raman scattered light was analyzed with a Spex 1403 double monochromator.

The laser power was about 30 mW, and about 500 scans had to be averaged to produce a suitable signal to noise ratio. The spectra were recorded with a resolution of about 4 cm^{-1} and an accuracy of 2 cm^{-1}. The loading of Ru was about 5 wt%.

2.9. ^{13}CO exchange reaction and alkylation

The studies on the ^{13}CO isotopic exchange reaction and alkylation of CH_3I and CH_3Li were done by IR spectroscopy. After deposition of **1** on the disk of oxides, the reactants such as ^{13}CO (30 Torr), CH_3I (80 Torr), and CH_3Li (30 Torr) were introduced into the IR cells at room temperature, and the sample spectra were recorded by IR at the same time.

2.10. Hydroformylation of ethylene

The ethylene hydroformylation was carried out using an open-flow mode reaction at 345–473 K. A mixture gas of ethylene, CO and H_2 (1:1:1 molar ratio at a pressure of 1×10^5 Pa) was passed through the catalyst bed (1 g of catalyst, Ru loading 1 wt%) at a flow rate of 60 ml/min. The samples were reduced for 2 h at 573 K in flowing H_2, followed by passing the mixture gas (ethylene, CO, and H_2) through the catalyst bed. The oxygenated products such as propanol and propaldehyde were collected in a water condenser (50 ml of water) by bubbling the effluent gas. The analysis of ethylene was performed by a Shimadzu GC-8AIT gas chromatograph with a thermal conductivity detector, using a 4 mm × 4 m porapak Q column at 343 K. The concentration of gas products in the off-gas was calibrated with an external standard by using 5 ml of gas sample. The analysis of propanol and propaldehyde dissolved in the water trap was conducted by a Shimadzu GC-8APF gas chromatograph with a flame ionization detector. Ethanol was added as an internal standard to calibrate the concentration of propanol and propaldehyde. In each gas chromatography the amount of the products was calculated with an integrator (CR-6A, Shimadzu).

3. Results and discussion

3.1. MgO-supported Ru ketenylidene cluster

The symmetry of **1** in its solid state is approximately C_{3V} with a set of three bridging CO ligands lying roundly in the plane of the metals and two sets of three terminally bound CO ligands arranged above and below the plane of the metals. The C–C and C–O bond distances of the symmetrically capping CCO group of triruthenium ketenylidene cluster are 1.30 and 1.17 Å, respectively; average M-terminal CO carbonyl distance is 1.87 Å; average M-bridging CO carbon distance is 2.11 Å [9].

The spectrum of MgO_{473} (Fig. 1a) showed a broad band at 3300–3800 cm^{-1}, and several bands at 1570–1350 cm^{-1}, which were as-

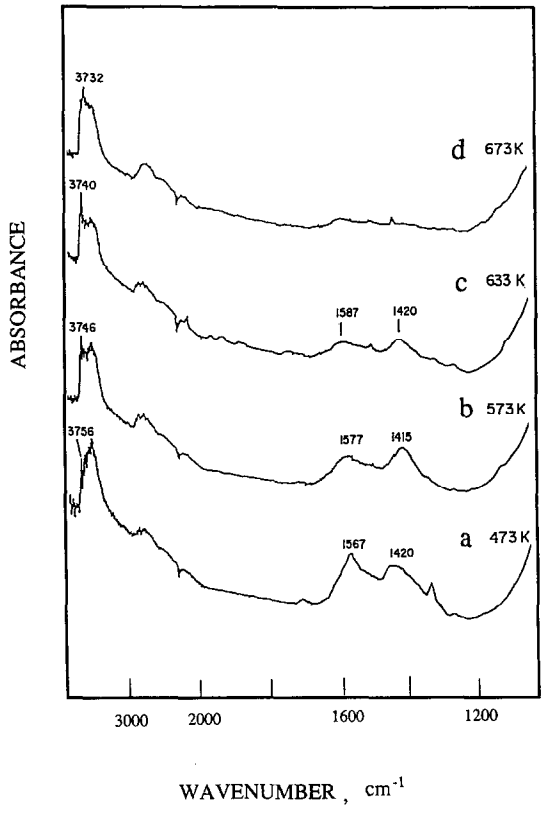

Fig. 1. IR spectra of MgO dehydrated for 2 h at (a) 473 K, (b) 573 K, (c) 633 K, and (d) 673 K.

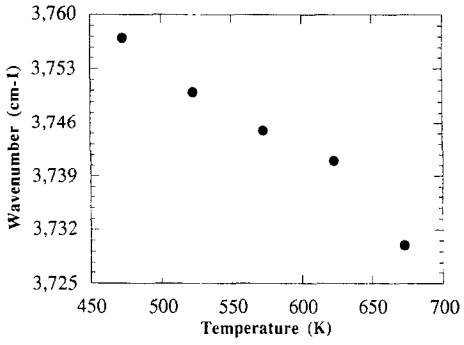

Fig. 2. Plots of OH frequencies versus dehydration temperature of MgO.

signed to Mg–OH, hydrogen-bonding and physical adsorption of water, and carbonate species, respectively [15–17]. Increasing the dehydration temperature to 573 K resulted in the partial elimination of physisorbed water and carbonates, giving the 3746 cm^{-1} band (MgO_{573}, Fig. 1b). A further increase of dehydration temperature up to 673 K led to the complete disappearance of carbonates (MgO_{673}). The spectrum included the band at 3732 cm^{-1}, assigned to terminal OH groups of the MgO support (Fig. 1d). Fig. 2 showed the hydroxyl frequency versus the dehydration temperature on the surface of MgO, indicating that the ν_{OH} decreased with the dehydration temperature. Based on the formula [15–17] $(2\pi\nu)^2 = K/M$, where ν and K stand for frequency and the constant of the OH binding energy, the lower frequency of OH groups indicated stronger acidity. Thus, it was suggested that the acidity of terminal OH groups of the MgO support increased with dehydration temperature.

When cluster **1** was deposited on the surface of $MgO_{473-573}$ (**1**/MgO, species I), the sample spectra exhibited very sharp bands at 2020, 1976, 1945, 1990 and 1752 cm^{-1} (Fig. 3(a, b), which are the same as those of **1** in CH_2Cl_2 (Table 2) [9,10]. The bands at 3746–3756 cm^{-1} (Fig. 3(a, b) assigned to OH groups of the MgO surface still keep their intensity, which indicated that there was no interaction between OH groups and triruthenium ketenylidene cluster. These results suggested that **1** was simply physisorbed on the surface of MgO.

When the cluster was deposited on $MgO_{633-673}$, the sample spectra (Fig. 3(c, d) included not only the bands appearing in Fig. 3a but also the new bands appearing at 2068, 2030, and 1999 cm^{-1} (**2**/MgO, species II) in Fig. 3(c, d). The new bands were assigned to the formation of **2** converted from **1** on the MgO surface. The major reasons were the following: (a) the species II appearing at 2068, 2030, and 1999

Table 1
Carbonyl frequencies of triruthenium ketenylidene species supported on MgO, SiO_2, SiO_2–Al_2O_3 supports

1/$MgO_{473-573}$ (species I)	**2**/$MgO_{573-673}$ (species II)	**2**/SiO_2 (species III)	**3**/SiO_2–Al_2O_3 (species IV)
			2124 (vw)
			2088 (s)
	2068 (w)	2068 (w)	2060 (vs)
			2040 (m)
	2030 (m)	2036 (s)	
2020 (m)			
			2010 (w)
	1999 (s)	2000 (vs)	
1976 (s)	1978 (vs)	1974 (m)	
1945 (vs)			
		1925 (vw)	
1890 (s)			
1800 (vw)			
1750 (s)			

vs = very strong, s = strong, m = middle, w = weak, vw = very weak. Unit is wavenumber (cm^{-1}).

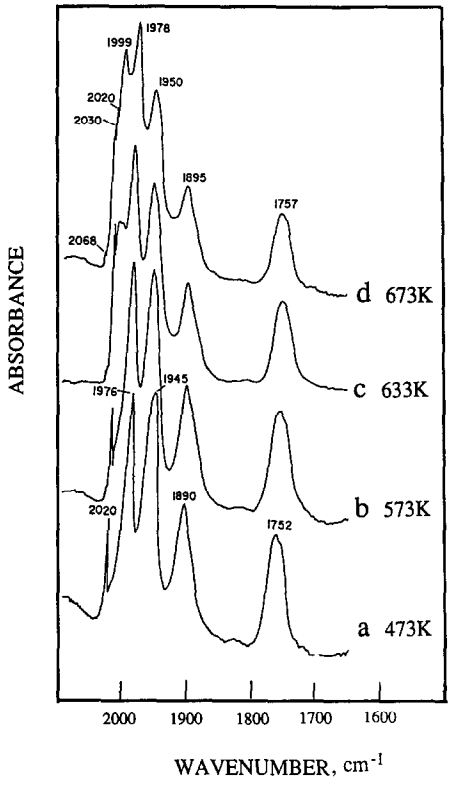

Fig. 3. IR carbonyl bands of $[PPN]_2[Ru_3(CO)_9(\mu_3\text{-}CCO)]$ (**1**) deposited on MgO dehydrated at (a) 473 K, (b) 573 K, (c) 633 K, and (d) 673 K.

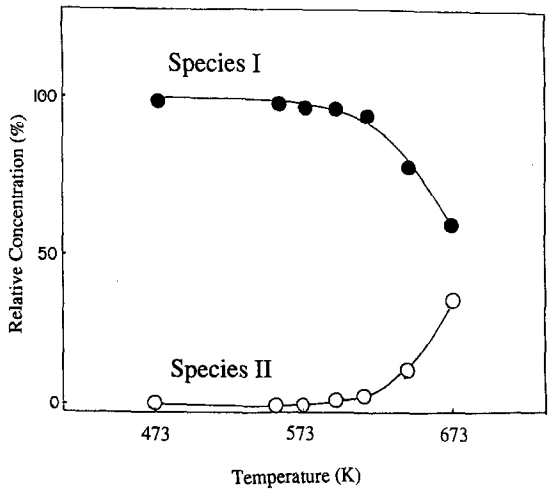

Fig. 4. The change in the concentration of species I (**1**) and species II (**2**) on MgO dehydrated at 473–673 K.

cm^{-1} were very closed to those of **2** in Tables 1 and 2; (b) the 1750 cm^{-1} band decreased with increasing bands at 2030 and 1999 cm^{-1}, which was the characteristic band of **1** in Tables 1 and 2; (c) bands at 3732–3740 cm^{-1} assigned to OH groups decreased significantly in intensity as a result of the deposition of **1** on MgO; (d) the acidity of OH groups increased with dehydration temperature on $MgO_{633-673}$; (e) **1** protonated on the metal frame to yield **2** in the solution [9,10].

As shown in Fig. 4, plots of infrared carbonyl intensity of surface species I and species II versus dehydration temperature gave the curves in the region from 473 to 673 K, indicating that

Table 2
Carbonyl frequencies [10] of various triruthenium ketenylidene clusters in different solvents

$[PPN]_2[Ru_3(CO)_9(\mu_3\text{-}CCO)]$ (**1**) in CH_2Cl_2	$[PPN][HRu_3(CO)_9(\mu_3\text{-}CCO)]$ (**2**) in Et_2O	$H_2Ru_3(CO)_9(\mu_3\text{-}CCO)$ (**3**) in hexane
		2123 (vw)
		2088 (s)
	2068 (w)	2062 (vs)
		2043 (m)
	2032 (s)	
2022 (m)	2017 (w)	
		2010 (w)
	1999 (vs)	
1980 (s)	1969 (m)	1969 (w)
1951 (vs)		
	1927 (vw)	
1898 (s)		
1800 (vw)		
1750 (s)		

vs = very strong, s = strong, m = middle, w = weak, vw = very weak. Unit is wavenumber (cm^{-1}).

species I was stoichiometrically converted into species II with increasing dehydration temperature. We suggest that **1** reacted with OH groups, as follows:

$$[Ru_3(CO)_6(\mu-CO)_3(\mu_3-CCO)]^{2-}$$
$$(\mathbf{1}, \text{species I}) + Mg\text{–}OH$$
$$= [HRu_3(CO)_9(\mu_3-CCO)]^- \{MgO^-\}$$
$$(\mathbf{2}, \text{species II}). \qquad (A)$$

3.2. SiO_2-supported Ru ketenylidene cluster

When **1** was deposited on SiO_2 at room temperature, the sample spectrum gave carbonyl bands at 2068, 2036, 2000, 1974, and 1925 cm^{-1} (species III in Fig. 5), which are consistent with those of **2** in Et_2O (Table 2) [10]. Also, the ν_{OH} band at 3740 cm^{-1} assigned to an isolated Si–OH group significantly decreased as a result of the adsorption of the cluster on the SiO_2 support, suggesting that there was a reaction of **1** with surface Si–OH groups.

It is of interest to find that the resulting material gave the band at 694 cm^{-1} in Fig. 6b. Some transition metal hydride carbonyl cluster complexes having a bending metal hydride bond typically exhibited a weak band (in-plane, M–H) in the region of 1100 to 1500 cm^{-1}, while out-of-plane bending modes of M–H–M appeared at 700 cm^{-1} [18–22] e.g. the band at 693 cm^{-1} (Fig. 6c) for the adsorption of $[Ru_3(CO)_{12}]$ on SiO_2 was attributed to the out-of-plane bending of Ru–H–Ru [22]. Therefore, the band at 694 cm^{-1} in Fig. 6b may be assigned to the out-of-plane bending mode of Ru–H–Ru. This result confirmed the formation of hydride triruthenium ketenylidene cluster on the SiO_2 support. Therefore, it was suggested that the complete transformation from **1** to **2** by reaction with Si–OH groups occurred as follows:

$$[Ru_3(CO)_6(\mu-CO)_3(\mu_3-CCO)]^{2-} \ (\mathbf{1})$$
$$+ \text{Si–OH} = [HRu_3(CO)_9(\mu_3-CCO)]^-$$
$$\{SiO^-\}(\mathbf{2}, \text{species III}). \qquad (B)$$

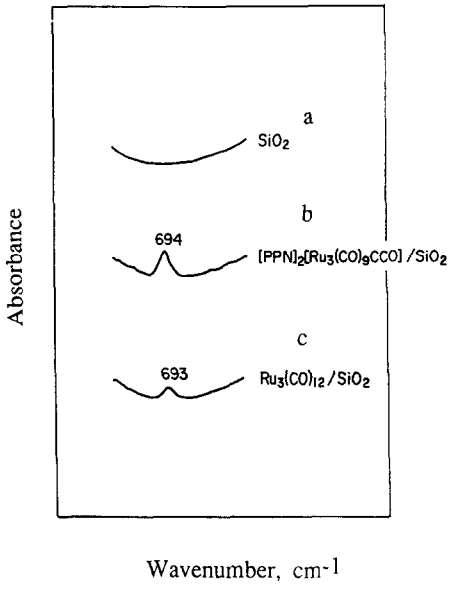

Fig. 6. IR spectra of (a) SiO_2, (b) deposition of $[PPN]_2[Ru_3(CO)_9(\mu_3\text{-CCO})]$ (**1**) on SiO_2, and (c) deposition of $[Ru_3(CO)_{12}]$ on SiO_2 in the region from 650 to 720 cm^{-1}.

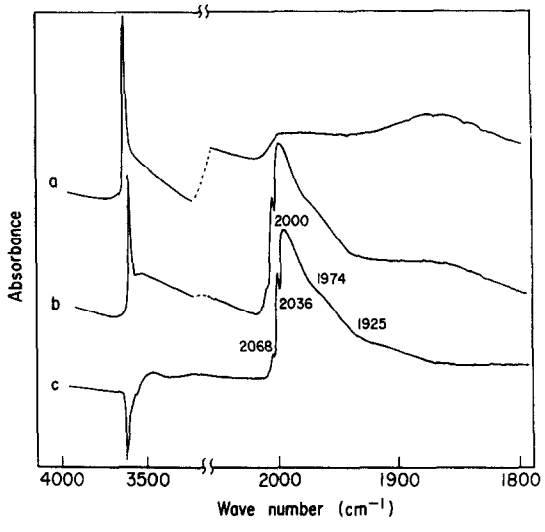

Fig. 5. IR spectra of carbonyl and hydroxyl bands of $[PPN]_2[Ru_3(CO)_9(\mu_3\text{-CCO})]$ (**1**) deposited on SiO_2 disk: (a) background of SiO_2, (b) the deposition of the cluster on SiO_2 and followed by evacuation for 0.5 h at room temperature, (c) difference spectrum (b − a).

3.3. SiO_2–Al_2O_3-supported Ru ketenylidene cluster

When **1** was deposited on strong acidic support of SiO_2–Al_2O_3, the sample spectrum (species IV in Fig. 7b) in the carbonyl region exhibited bands at 2124, 2088, 2060, 2010, and 2010 cm^{-1}, and several weak bands lower than 2000 cm^{-1}, which are very close to those of **3** in hexane (Table 2) [10]. The H-type of SiO_2–Al_2O_3 showed two bands at 3740 and 3620 cm^{-1} (Fig. 7a), which were assigned to Si–OH and Si(OH)Al, respectively [23,24]. The band at 3620 cm^{-1} decreased remarkably in intensity as a result of the deposition of the cluster onto the SiO_2–Al_2O_3 support, while the band at 3740 cm^{-1} kept its intensity (Fig. 7(b, c), indicating that cluster **1** selectively reacted with 3620 cm^{-1} species.

It has been reported that there are two types

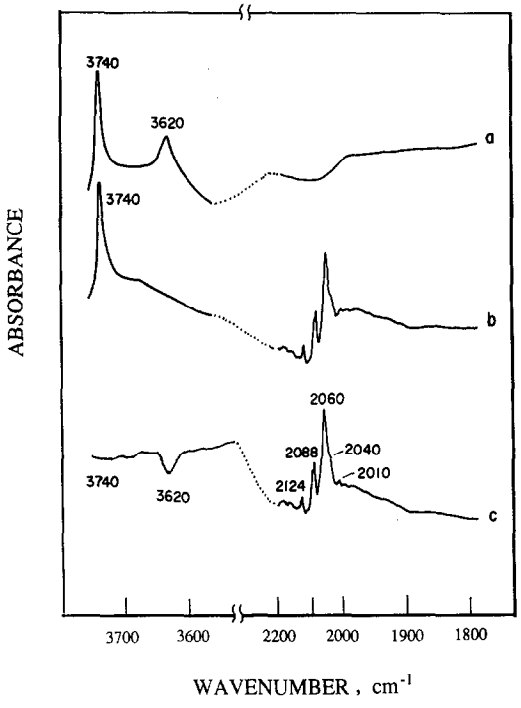

Fig. 7. IR spectra of carbonyl and hydroxyl bands of $[PPN]_2[Ru_3(CO)_9(\mu_3\text{-}CCO)]$ (**1**) deposited on SiO_2–Al_2O_3 disk: (a) background of SiO_2–Al_2O_3, (b) the deposition of the cluster on SiO_2–Al_2O_3, followed by evacuation for 0.5 h at room temperature, (c) difference spectrum (b − a).

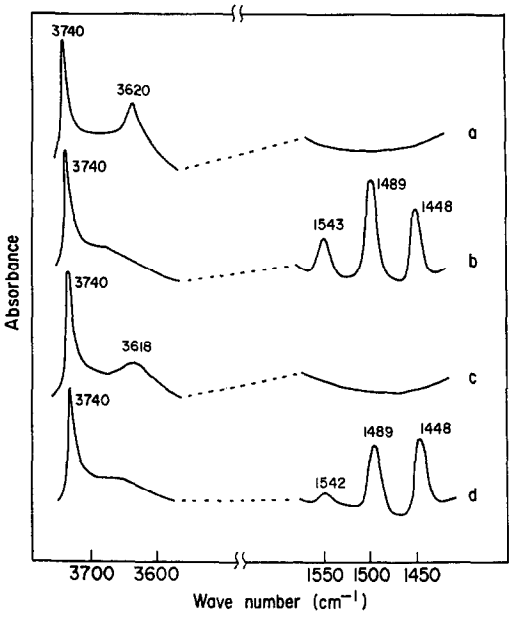

Fig. 8. IR spectra of carbonyl and hydroxyl bands associated with the adsorption of pyridine: (a) evacuation of SiO_2–Al_2O_3 for 2 h at 573 K, (b) after (a), the adsorption of 10 Torr of pyridine for 1 h at room temperature and evacuation for 1 h at 433 K, (c) the deposition of $[PPN]_2[Ru_3(CO)_9(\mu_3\text{-}CCO)]$ (**1**) on SiO_2–Al_2O_3 disk, (d) after (c), adsorption of 10 Torr pyridine for 1 h at room temperature and evacuation for 1 h at 433 K.

of stronger acidic sites, Brønsted sites and Lewis sites, on the surface of the SiO_2–Al_2O_3 support. There was a possibility that the surface reaction may due to either the Ru cluster with Brønsted sites or the Ru cluster with Lewis sites.

Fig. 8 showed adsorption of pyridine on SiO_2–Al_2O_3 and on the SiO_2–Al_2O_3-supported triruthenium ketenylidene cluster. When the SiO_2–Al_2O_3 disk was evacuated for 2 h at 573 K, the sample spectrum (Fig. 8a) exhibited two sharp bands at 3740 and 3620 cm^{-1} [23,24]. Exposure of 10 Torr of pyridine to the SiO_2–Al_2O_3 disk at room temperature led to complete disappearance of the band at 3620 cm^{-1}, but the band at 3740 cm^{-1} was unchanged. In the region of C–C bending–stretching frequencies, three strong bands at 1543, 1489, and 1448 cm^{-1} were observed (Fig. 8b). The band at 1543 cm^{-1} was assigned to C–C stretching vibration of the pyridinium ion and is com-

monly used for detecting the presence of Brønsted acidic sites, and the band at 1448 cm^{-1} was attributed to adsorption of pyridine on Lewis acidic sites [25]. Notably, the spectrum of pyridine adsorbed on the sample of the SiO_2–Al_2O_3-supported Ru ketenylidene cluster also included the three bands at 1542, 1498, and 1448 cm^{-1}, but the band intensities were different. As compared with those in Fig. 8b, in Fig. 8d the band intensity at 1542 cm^{-1} was markedly reduced, while the band intensity at 1448 cm^{-1} basically remained, suggesting that the Lewis acidic sites on the SiO_2–Al_2O_3 support did not react with the triruthenium ketenylidene cluster.

These results indicated that the species IV resulted from the surface reaction of **1** with Si(OH)Al groups on the surface of SiO_2–Al_2O_3 as follows:

$$[Ru_3(CO)_6(\mu-CO)_3(\mu_3-CCO)]^{2-}\ (\mathbf{1}) + 2Si(OH)Al = H_2Ru_3(CO)_9(\mu_3-CCO)] \times 2\{Si(O^-)Al\}\ (\mathbf{3}, \text{species IV}). \quad (C)$$

3.4. Extraction and yield determination

The infrared spectra of the liquid extracted from MgO_{573} supported **1** (species I) in the ν_{CO} region included the bands at 2024, 1979, 1951, 1898, and 1750 cm^{-1} (Fig. 9b), which are the same as those of **1** in CH_2Cl_2 solvent (Fig. 9a, 2022, 1979, 1951, 1897, and 1750 cm^{-1}).

The extracted solution obtained from SiO_2-supported triruthenium ketenylidene cluster (species III) in the ν_{CO} region included the bands at 2068, 2030, 2000, 1968 and 2926 cm^{-1} (Fig. 10b), in good agreement with those of **2** in Et_2O solvent (Fig. 10a, 2069, 2033, 2000, 1969, 1927 cm^{-1}).

The solution extracted from the SiO_2–Al_2O_3 supported triruthenium ketenylidene cluster (species IV) in the ν_{CO} region included the bands at 2119, 2083, 2056, 2039, 2011, 2003, and 1993 cm^{-1} (Fig. 11b). The spectrum closely matched that of **3** in hexane (Fig. 11a, 2118,

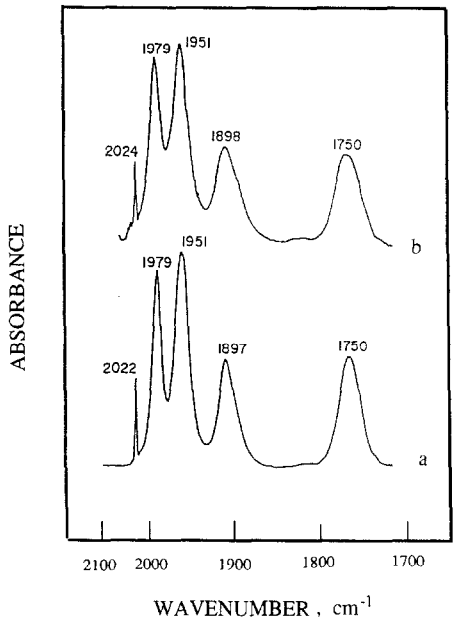

Fig. 9. IR spectra of (a) the solution from extraction of MgO-supported triruthenium ketenylidene cluster (species I) by use of CH_2Cl_2 solvent, and (b) $[PPN]_2[Ru_3(CO)_6(\mu CO)_3(\mu_3\text{-}CCO)]$ (**1**) in CH_2Cl_2 solvent.

2085, 2056, 2040, 2005, 1995, and 1962 cm^{-1}).

Also, NMR ^{13}C spectra of solution extracted from oxide species were the same as those of the clusters in solvents, which confirmed that the clusters of **1**, **2**, and **3** were selectively formed on the surface of MgO, SiO_2, and SiO_2–Al_2O_3 dehydrated at 573 K, respectively.

To determine the yield of SiO_2- and SiO_2–Al_2O_3-supported triruthenium ketenylidene clusters, the solution formed by extraction with [PPN]Cl of oxide-supported surface species was filtered through a medium-porosity glass frit in the presence of N_2, and the powder was washed with the solvent and filtered again through the frit. The resultant solution was evacuated to get solid powder. The yield of **2** on SiO_2 (species III) and **3** on SiO_2–Al_2O_3 (species IV) was 94% and 90%. In contrast, the yield of **2** and **3** prepared from the solution synthesis was only 41% and 45%, respectively [10].

It is apparent that the preparation of oxide-supported ruthenium ketenylidene cluster (*surface-mediated organometallic synthesis*) exhibited the following obvious features: (a) higher

product yield for the synthesis of **2** and **3** complexes; (b) simpler than that of the solution synthesis; e.g. the synthesis of **2** in the solution at low temperature (198 K) took for several hours, and the surface-mediated synthesis at room temperature took for 30 min; (b) easier purification by extraction from the surface; (d) the synthesis variables including the nature and loading of the metal salt or organometallic precursor adsorbed on solid, the physical properties of the solid, the chemical properties of the surface, the gas atmosphere, temperature, and pressure. Recently, Gates et al. [26–31] have successfully synthesized a series of metal carbonyl clusters such as iridium carbonyl, osmium carbonyl, rhodium carbonyl, and platinum carbonyl by using surface-mediated organometallic synthesis.

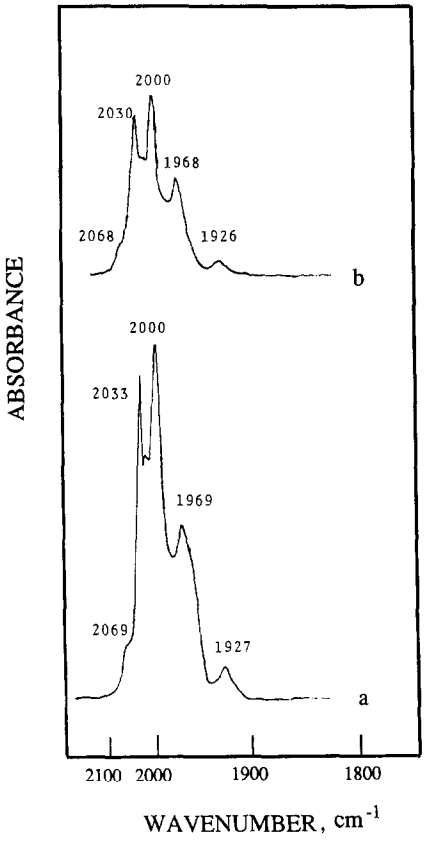

Fig. 10. IR spectra of (a) the solution from extraction of SiO_2-supported triruthenium ketenylidene cluster (species III) by use of Et_2O solvent, and (b) [PPN][$HRu_3(CO)_9(\mu_3$-CCO)] (**2**) in Et_2O solvent.

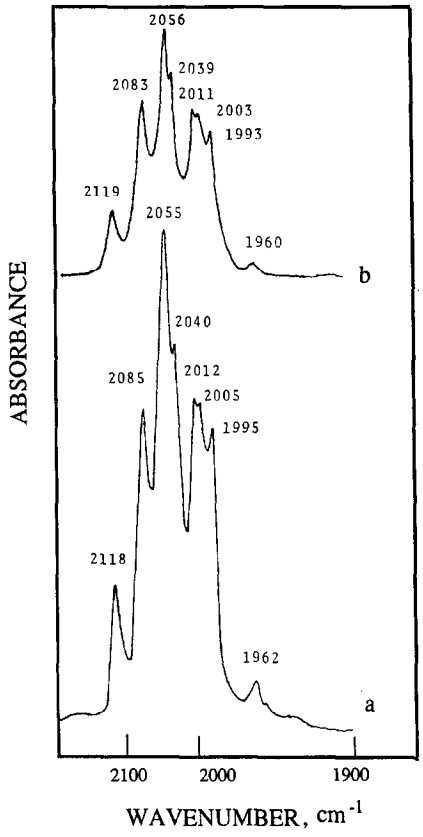

Fig. 11. IR spectra of (a) the solution from extraction of SiO_2–Al_2O_3 supported triruthenium ketenylidene cluster (species IV) by use of hexane, and (b) $H_2Ru_3(CO)_9(\mu_3$-CCO) (**3**) in hexane.

3.5. Raman spectroscopy of Ru ketenylidene clusters on MgO_{573} and SiO_2

The Raman technique is potentially valuable for determining the structures of supported-metal clusters since it has been used to demonstrate metal–metal bonding in a wide range of molecular metal clusters [32]. In particular, it determines whether the structures of metal clusters can exist on the surface of oxide supports. Because of the high fluorescence, low sensitivity, and decomposition of metal clusters [1], there were a number of experimental difficulties. Since the metal–metal vibrations fortunately have rather high Raman scattering cross sections, researchers can use a low power laser line and sample spinning cell techniques to obtain the suitable signal of metal–metal bond-

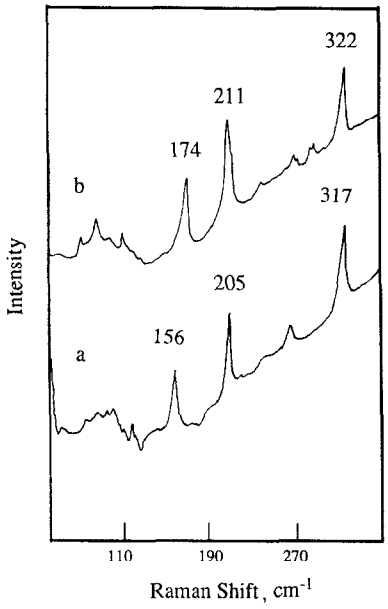

Fig. 12. Raman spectra of $[PPN]_2[Ru_3(CO)_6(\mu\text{-}CO)_3(\mu_3\text{-}CCO)]$ (**1**) on (a) MgO and (b) SiO_2 at room temperature.

ing. Several examples of Raman research dealing with oxides-supported metal carbonyl clusters have been reported [33–36]. Generally, at frequencies lower than 350 cm^{-1}, several vibrations were expected to be active in the Raman spectra of metal clusters, which were related to the Ru–Ru, Ru–C, and Ru–O stretching modes.

Fig. 12 showed the Raman spectra of **1** on MgO and SiO_2 in the region from 30 to 350 cm^{-1}. For the MgO-supported **1**, we observed three bands at 156, 205, and 317 cm^{-1}, with broad and shoulder bands appearing at lower frequencies (Fig. 12a). The bands at 156 and 205 cm^{-1} were proposed to belong to Ru–Ru stretching modes, and the band at 317 cm^{-1} was proposed to belong to the Ru_3–C stretching mode, respectively. These assignments are in good agreement with those of **1** in CH_2Cl_2 solvent [37]. The Raman band position between the MgO_{573}-supported cluster and the cluster in CH_2Cl_2 was almost the same. The difference was only for band intensity, which was really contributed by a small amount of the cluster on the surface of MgO_{573}. These results demonstrate that the symmetry between the cluster on MgO and the cluster in CH_2Cl_2 was the same, indicating that the cluster physisorbed on the surface of the MgO support.

On SiO_2-supported triruthenium ketenylidene cluster (Fig. 12b), the Raman spectrum gave rise to bands at 174, 211, and 322 cm^{-1}, with weak and broad bands at 40–110 cm^{-1} (Fig. 12b). The bands at 174 and 211 cm^{-1} were assigned to Ru–Ru stretching modes and the band at 322 cm^{-1} was assigned to the Ru_3–C stretching mode; these are in good consistence with those of **2** in CH_2Cl_2 [37]. The weak and broad bands at lower frequencies were tentatively assigned to Ru–C bending modes, in agreement with those of $[Ru_3(CO)_{12}]$ [38]. Comparatively, there was an approximate 20 cm^{-1} shift for Raman spectra in the Ru–Ru stretching between MgO- and SiO_2-supported triruthenium ketenylidene clusters, which may be explained by the various surface species possibly assigned to **1** on MgO (species I) and **2** on SiO_2 (species III), respectively.

3.6. ^{13}CO exchange reaction

When ^{13}CO at 15 Torr was exposed to MgO_{573}-supported **1** (species I), we could not observe any new bands due to isotopic effects, even at temperatures up to 523 K (Fig. 13). The decrease in intensity of the ν_{CO} band was attributed to the decarbonylation of the ruthenium ketenylidene cluster, indicating a negligible activity for the isotopic exchange reaction.

When ^{13}CO at 15 Torr was exposed to SiO_2-supported triruthenium ketenylidene cluster (**2**, species III) for 2 h at room temperature, the bands at 2036 and 2000 cm^{-1} were reduced, and a strong band appeared at 1996 cm^{-1} due to ^{13}CO isotopic exchange reactions (Fig. 14b). The result was interpreted by the little amount of CO ligands exchanged by ^{13}CO, and a lot of carbonyls were still CO. The IR band of CO overlapped with that of ^{13}CO, giving the band at 1996 cm^{-1}. As the temperature was increased to 433 K, the major band was shifted to 1990 cm^{-1} (Fig. 14c). The difference spectra (Fig.

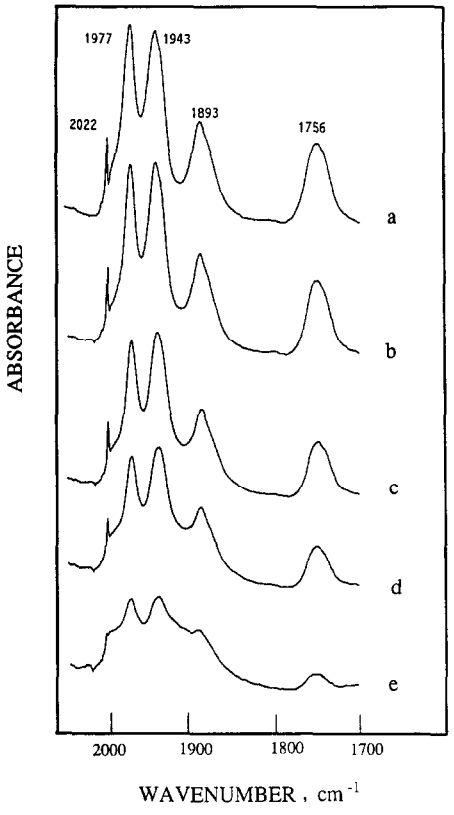

Fig. 13. IR spectra of carbonyl bands on MgO (dehydration at 573 K) supported on $[PPN]_2[Ru_3(CO)_6(\mu\text{-}CO)_3(\mu_3\text{-}CCO)]$ (1) (species I): (a) before exposure to ^{13}CO at room temperature, (b) after (a), 15 Torr ^{13}CO for 13 h at room temperature, (c) after (b), 2 h at 353 K, (d) after (c), 2 h at 403 K, (e) after (d), 2 h at 473 K.

14(d, e) between before and after isotopic exchange showed that the bands at 2030–1990 cm^{-1} decreased in intensity as a result of the increase of the bands at 1975–1940 cm^{-1}. The major band was shifted to 1990 cm^{-1} (Fig. 14c), which may be explained by (a) more CO being exchanged with ^{13}CO and (b) partial decarbonylation occurring at increased temperature. These results indicated that SiO_2-supported **2** exhibited some reactivity in ^{13}CO exchange reactions, but the rate was very slow.

When ^{13}CO at 15 Torr was exposed to SiO_2–Al_2O_3-supported triruthenium ketenylidene cluster (**3**, species IV) for 2 h at room temperature, the bands at 2130 and 2060 cm^{-1} were markedly decreased, a new band appeared at 2016 cm^{-1} due to isotopic effects, while the band at 2100 cm^{-1} basically remained its intensity (Fig. 15c). As the temperature was ramped to 323 K, the band at 2128 cm^{-1} completely disappeared, and the bands at 2098 and 2056 cm^{-1} considerably decreased with a slight shift downward, as compared with those for the sample spectrum at room temperature (Fig. 15d). It was suggested that the bands at 2138 and 2060 cm^{-1} and at 2100 cm^{-1} in Fig. 15a were attributed to different types of carbonyl ligands, which have different activities in the isotopic exchange reaction. The assignment of various types of carbonyls required further experiments. When the temperature was increased to 373 K, all bands in Fig. 15a disappeared. As a result, a series of new bands at 2078, 2050, and 2010

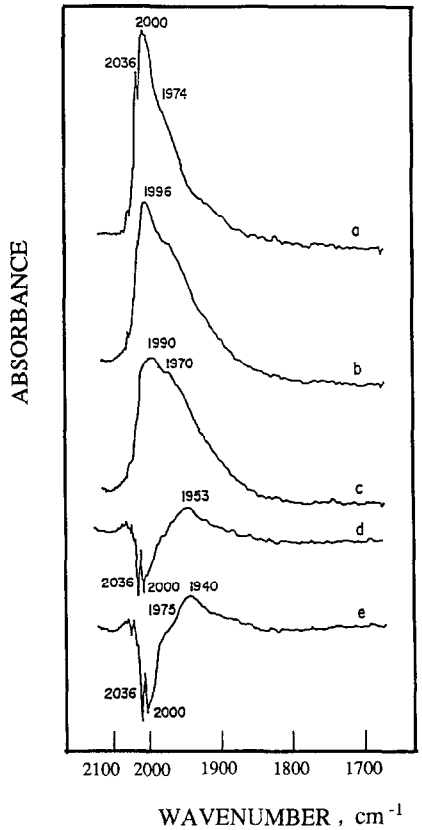

Fig. 14. IR spectra of carbonyl bands on SiO_2 supported on $[PPN][HRu_3(CO)_9(\mu_3\text{-}CCO)]$ (**2**) (species III): (a) before exposure to ^{13}CO at room temperature, (b) after (a), 15 Torr ^{13}CO for 2 h at room temperature, (c) after (b), 2 h at 443 K, (d) difference spectrum (b − a), (e) difference spectrum (c − a).

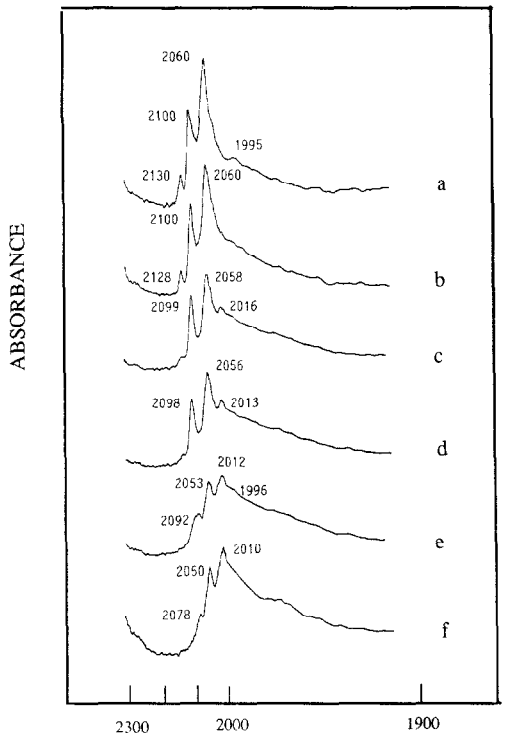

Fig. 15. IR spectra of carbonyl bands on SiO_2–Al_2O_3 supported on $H_2Ru_3(CO)_9(\mu_3\text{-}CCO)$ (**3**) (species IV): (a) before exposed to ^{13}CO at room temperature, (b) after (a), 15 Torr ^{13}CO for 1 h at 120 K, (c) after (b), 2 h at room temperature, (d), after (c), 2 h at 323 K, (e) after (d), 2 h at 353 K, (f) 2 h at 373 K.

cm^{-1} appeared (Fig. 15f), which are in good agreement with theoretical frequencies [39] for 2130, 2100, and 2060 cm^{-1} (Fig. 15a) in CO isotopic exchange reactions, indicating that the isotopic exchange was complete. The results showed that the isotopic exchange on $SiO_2Al_2O_3$-supported **3** (species IV) was very active as compared with SiO_2-supported **2**.

A summary of the above results shows the reaction order for the isotopic exchange to be $\mathbf{1}/MgO \ll \mathbf{2}/SiO_2 \ll \mathbf{3}/SiO_2$–$Al_2O_3$. In general, the mechanism of ^{13}CO and CO isotopic exchange reactions on metal particles is as follows [39]:

$$RuCO + {}^{13}CO \rightarrow O^{13}CRuCO \text{ (intermediate)} \rightarrow O^{13}CRu + CO. \quad \text{(D)}$$

This mechanism suggests that there was an intermediate in the isotopic exchange reactions and that the activity has a good relationship to the rate of CO adsorption–desorption on the metal surface. It is obvious that the activity in CO isotopic exchange will become slow if the CO–metal bonding is increased.

The three triruthenium ketenylidene clusters had the same metal framework Ru_3, and the difference was only in the protons. The formation of hydrido clusters such as **2** and **3** would result in the increase of bonding orbitals and the decrease of electron density in bonding orbitals, as compared with **1**. These analyses suggest that the bonding between carbonyl ligands and the triruthenium frame in **2** and **3** was much lower than that in **1** [40,41], giving a higher activity for ^{13}CO isotopic exchange and a higher frequency for carbonyl ligands, which is good in agreement with experimental facts (Figs. 13–15).

3.7. Alkylation with CH_3I and CH_3Li

Although MgO_{573} supported on **1** (species I) was inactive for ^{13}CO isotopic exchange, it was very active for the alkylation with CH_3I, similar to the chemistry in solution [10]. When CH_3I (80 Torr) and CO (80 Torr) were introduced onto the sample disk of species I in the IR cell at room temperature, the bands at 1977, 1943, 1984, and 1756 cm^{-1} gradually decreased with the appearance of a series of new bands at 2960, 1635, 1462, and 1350 cm^{-1} (Fig. 16).

In solution chemistry, Shriver et al. [10] reported that the dinegative clusters attack the CH_3I to produce the acetyl cluster. Here, it is proposed that similar alkylation occurred on the MgO-supported **1** (species I), because the resulting infrared spectra of the reaction on the surface species were similar to those in solution chemistry. Therefore, the band at 2960 cm^{-1} was assigned to the C–H stretching frequency of the $-CH_3$ group, the band at 1635 cm^{-1} was assigned to the C=O stretching frequency of the $-CC(O)CH_3$ group, and the bands at 1462 and

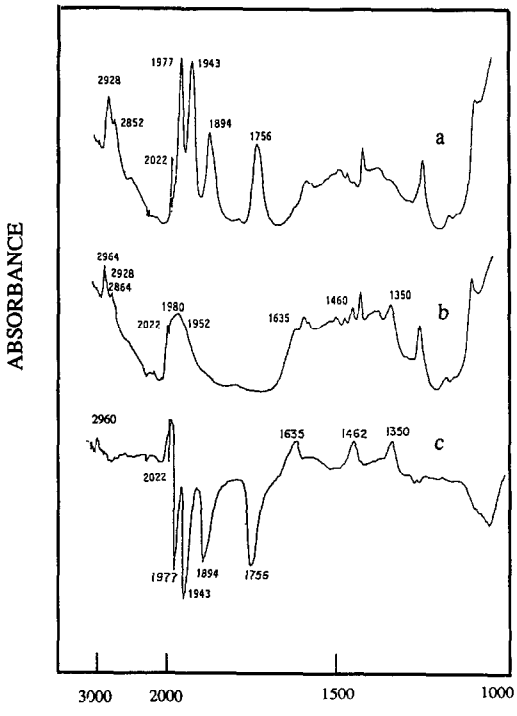

Fig. 16. IR spectra of MgO-supported $[PPN]_2[Ru_3(CO)_9(\mu_3\text{-}CCO)]$ (**1**) (species I) by reaction with CH_3I under CO at room temperature: (a) before reaction, (b), after (a), admission of 80 Torr CH_3I and evacuation for 1 h, (c) difference spectra (b − a).

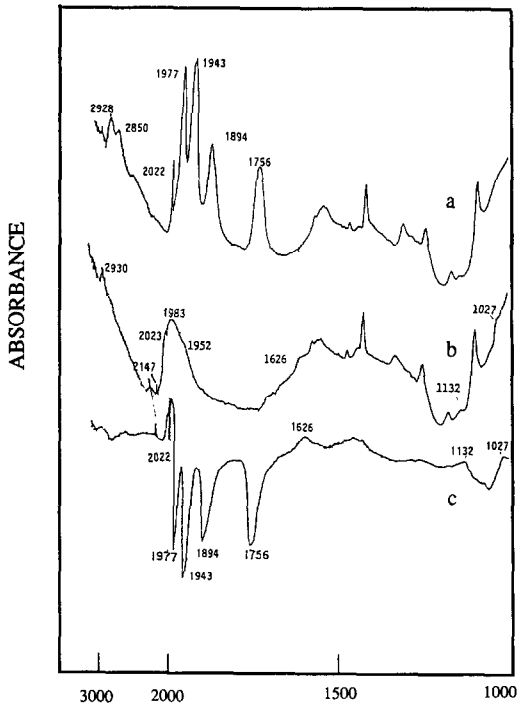

Fig. 17. IR spectra of MgO-supported $[PPN]_2[Ru_3(CO)_9(\mu_3\text{-}CCO)]$ (**1**) (species I) by reaction with CD_3I under CO at room temperature: (a) before reaction, (b), after (a), admission of 80 Torr CD_3I and evacuation for 1 h, (c) difference spectra (b − a).

1350 cm^{-1} were assigned to deformation modes of $-CH_3$ groups, which was confirmed by the D-labeled experiments. By using CD_3I instead of CH_3I, the sample spectra exhibited bands at 2147, 1626, 1132, and 1027 cm^{-1} (Fig. 17). We proposed that the band at 2147 cm^{-1} was assigned to the C–D stretching frequency of $-CD_3$ groups; The two bands at 1132 and 1027 cm^{-1} were assigned to the C–D deformation mode; the band at 1626 cm^{-1} was assigned to C=O stretching of the acyl moiety $C(O)CD_3$. These assignments are in good consistence with the theoretical value calculated from the isotopic effect [39]. Table 3 summarizes these assignments.

Reaction of SiO_2-supported on **2** (species III) with CH_3I at room temperature proceeded very slowly, but at 473 K it gave several new bands. By contrast, SiO_2–Al_2O_3-supported **3** (species IV) was completely inactive for the reaction with CH_3I, even for temperatures up to 573 K.

A change in alkylation reagent by using nucleophilic CH_3Li instead of electrophilic CH_3I

Table 3
Infrared bands [a] of MgO_{573}-supported triruthenium ketenylidene cluster with CH_3I or CD_3I under CO

CH_3I	CD_3I	Structure of group	Assignment
2960	2147	CH_3 or CD_3	asymmetric stretching of CH or CD
1635	1626	$-CC(O)CH_3$ or $-CC(O)CCD_3$	C=O stretching mode
1462	1132	CH_3 or CD_3	asymmetric deformation of CH or CD
1350	1027	CH_3 or CD_3	symmetric deformation of CH or CD

[a] Unit is wavenumber (cm^{-1}).

Table 4
Hydroformylation of ethylene on oxides-supported triruthenium ketenylidene cluster-derived catalysts [a]

Surface species	Rate of formation at 445 K [b]		Selectivity for oxygenates (mol%) [c]	Selectivity for alcohol (mol%) [d]
	C_2H_6	$C_2H_5CHO + C_3H_7OH$		
$[Ru_3(CO)_9(CCO)]^{2-}\{MgO\}$ (1)	30	11	27	46
$[HRu_3(CO)_9(CCO)]^{-}\{SiO^{-}\}$ (2)	55	3.5	6	0
$H_2Ru_3(CO)_9(CCO)2\{Si(O)^{-}Al\}$ (3)	120	2.0	2	0
MgO or SiO_2 or SiO_2–Al_2O_3	—	—	—	—

[a] Flow rate $C_2H_4/CO/H_2 = 20/20/20$ ml/min, total pressure is 1 atm.
[b] mmol/(mol Ru)/min.
[c] $(C_2H_5CHO + C_3H_7OH)/(C_2H_5CHO + C_3H_7OH + C_2H_6) \times 100\%$.
[d] $C_3H_7OH/(C_2H_5CHO + C_3H_7OH) \times 100\%$.

showed an opposite order over these supported clusters. At room temperature, the alkylation of SiO_2–Al_2O_3-supported **3** (species IV) proceeded with high rate. The SiO_2-supported **2** (species III) began to react with CH_3Li at nearly 363 K. Comparatively, the MgO_{573}-supported **1** (species I) does not react with CH_3Li, even at temperatures up to 573 K.

Comparison of various triruthenium ketenylidene clusters supported on oxides in alkylation of CH_3I and CH_3Li exhibited that the reactivity was strongly dependent on the surface species containing the number of protons as follows:

in reaction with CH_3I: $\mathbf{1}/MgO \gg \mathbf{2}/SiO_2 \gg \mathbf{3}/SiO_2$–$Al_2O_3$;

in reaction with CH_3Li: $\mathbf{3}/SiO_2$–$Al_2O_3 \gg \mathbf{2}/SiO_2 \gg \mathbf{1}/MgO$.

3.8. Ethylene hydroformylation

Before ethylene hydroformylation, we performed decarbonylation of various triruthenium ketenylidene clusters supported on oxides, and IR spectra indicated that all carbonyl infrared bands disappeared as the temperature was ramped from room temperature to 573 K over 1 h and then held at 573 K for 2 h.

The data of ethylene hydroformylation over these samples were summarized in Table 4. In all runs, the activity reached steady state after 5 h on stream and remained constant for the subsequent 55 h. Higher rates for propanal and 1-propanol were observed on MgO_{573}-supported **1** (species I) than on SiO_2- and SiO_2–Al_2O_3-supported **2** and **3** (species III and species IV). The rate for ethane was effectively suppressed on MgO_{573}. In contrast, the oxides such as MgO, SiO_2, and SiO_2–Al_2O_3 were completely inactive for the formation of ethane and oxygenates at the same conditions. The orders of activity and selectivity for ethane and oxygenates in the ethylene hydroformylation over various ruthenium ketenylidene clusters supported on oxides were the following:

activity for oxygenates: $\mathbf{1}/MgO > \mathbf{2}/SiO_2$, $\mathbf{3}/SiO_2$–Al_2O_3;

selectivity for alcohol: $\mathbf{1}/MgO > 2/SiO_2$, $\mathbf{3}/SiO_2$–Al_2O_3;

activity for ethane: $\mathbf{3}/SiO_2$–$Al_2O_3 > \mathbf{2}/SiO_2 > \mathbf{1}/MgO$.

Generally, the large difference in ethylene hydroformylation could be due to variation in the surface structure and active sites, which were related to changes in metal loading, metal dispersion, surface area and other preparation conditions. We know that the Ru loading is the same, the surface areas are similar, and these oxides are completely inactive for the ethylene hydroformylation. Therefore, the large difference in catalytic activity and selectivity might be due to the surface species having various properties.

The mechanism of ethylene hydroformylation on supported triruthenium cluster-derived catalysts [42,43] may include some of the following elementary steps: (a) the adsorption of CO, H_2, and ethylene occurred on the Ru sites; (b) hydrogenation of adsorbed ethylene gave an ad-

sorbed ethyl group; (c) hydrogenation of the adsorbed ethyl group produced ethane; (d) CO inserted into adsorbed hydrogen to form a formyl species; also, CO inserted into the adsorbed ethyl group to form a propionyl species; (e) the ethyl group reacted with the formyl species to produce a propionyl species; (f) hydrogenation of the propionyl group resulted in the formation of propaldehyde, and further hydrogenation of adsorbed propaldehyde gave propanol.

Considering the CO isotopic exchange reaction (Figs. 13–15), higher activity may indicate higher bonding of C–O and lower bonding of Ru–CO. The results imply that C–O bonding in **1** supported on MgO was much weaker than that of **3** supported on SiO_2–Al_2O_3. Thus, we suggest that C–O with weak bonding in **1** supported on MgO would be easily insertable into the bonding of ruthenium with hydrogen or/and ethyl species, exhibiting a high rate for oxygenated formation, as compared with that in **2** and **3** supported on SiO_2 and SiO_2–Al_2O_3.

In alkylation of CH_3I and CH_3Li, we observed that **1** supported on MgO was very active with electrophile agents while **3** supported on SiO_2–Al_2O_3 was very active with nucleophiles. When CO and ethylene adsorbed on Ru sites, the CO insertion in **1** supported on MgO may be faster than that in **3** supported on SiO_2–Al_2O_3 because the properties of adsorbed ethyl species are similar to that of the electrophile.

Furthermore, we found that the surface clusters with hydrides (**2** and **3**) exhibited very high activity for ethane formation as compared with that of **1** supported on MgO. The results may imply that hydride species in the clusters played an important role for the formation of ethane product. Possibly, the hydride species markedly promote catalytic activity in hydrogenation of the adsorbed ethyl group on Ru sites.

3.9. Support effect

Many researchers [1–5] have studied the catalytic performance on various supports, suggesting various models of support effects such as hydrogen-spillover and support-metal interaction. In the present study, we found that the deposition of **1** on oxides having different acid–base properties resulted in the formation of **1**/MgO, **2**/SiO_2, and **3**/SiO_2–Al_2O_3, respectively, which showed different activity and selectivity in CO isotopic exchange, alkylation, and catalytic hydroformation of ethylene. The support effect is apparent, and the acid–base properties of supports are very important for the formation of surface species.

4. Conclusions

The important conclusions of this study may be summarized as follows:

(i) The surface species of $[Ru_3(CO)_6(\mu\text{-}CO)_3(\mu_3\text{-}CCO)]^{2-}$ (**1**) supported on MgO, characterized by IR spectroscopy, strongly depended on dehydration temperature. At dehydration temperatures below 573 K, the sample cluster exhibited characteristic bands of $[Ru_3(CO)_6(\mu\text{-}CO)_3(\mu_3\text{-}CCO)]^{2-}$ (**1**). A new adspecies assigned to $[HRu_3(CO)_9(\mu_3\text{-}CCO)]^-$ (**2**) was characterized by the new bands at 2068, 2030, and 1999 cm^{-1} as the dehydration temperature was increased to 673 K.

(ii) On the SiO_2 support, the IR investigation suggested that the stoichiometric protonation of $[Ru_3(CO)_6(\mu\text{-}CO)_3(\mu_3\text{-}CCO)]^{2-}$ (**1**) with surface hydroxyl groups (Si–OH) occurred, giving $[HRu_3(CO)_9(\mu_3\text{-}CCO)]^-$ (**2**). Deposition of $[Ru_3(CO)_6(\mu\text{-}CO)_3(\mu_3\text{-}CCO)]^{2-}$ (**1**) on SiO_2–Al_2O_3 resulted in selective formation of $H_2Ru_3(CO)_9(\mu_3\text{-}CCO)$ (**3**) by reaction with strong *Brønsted* acidic groups of Si(OH)Al.

(iii) The IR spectra of the solution extracted from surface species confirmed selective formation of dinegative monohydride and dihydride species on MgO_{573}, SiO_2, and SiO_2–Al_2O_3, respectively. Notably, the yield of $[HRu_3(CO)_9(\mu_3\text{-}CCO)]^-$ (**2**) and $H_2Ru_3(CO)_9(\mu_3\text{-}CCO)$ (**3**) prepared from *surface-mediated synthesis* was 94% and 90%,

Table 5
Characterization and reactivities of triruthenium ketenylidene clusters on oxides in the CO isotopic exchange reaction, alkylation of CH_3I and CH_3Li, and hydroformylation of ethylene

Support	MgO_{573}	SiO_2	SiO_2–Al_2O_3
Deposition of triruthenium ketenylidene cluster on oxide	species I	species III	species IV
Assignment	$[Ru_3(CO)_9(CCO)]^{2-}$ {MgO} (1)	$[HRu_3(CO)_9(CCO)]^-$ {SiO^-} (2)	$H_2Ru_3(CO)_9(CCO)$ {Si(O)$^-$Al} (3)
Characterization	IR, extraction, Raman	IR, extraction, Raman	IR, extraction
Isotopic exchange of ^{13}CO	− − − − [a]	+ + [b]	+ + + +
Alkylation with CH_3I	+ + + + +	+	− − − −
Alkylation with CH_3Li	− − − −	+	+ + + +
Ethylene hydroformylation			
Formation of oxygenates	+ + + +	+ +	+
Formation of ethane	+	+ +	+ + + + +
Selectivity for alcohols	+ +	−	−

[a] '−': inactive.
[b] '+': active.

much higher than those prepared from *solution synthesis*.

(iv) Raman spectra of MgO_{573} and SiO_2 supported on triruthenium ketenylidene clusters exhibited bands at 156, 205 and 317 cm^{-1}, and 174, 211 and 322 cm^{-1}, respectively, which were tentatively assigned to Ru–Ru and Ru_3–C stretching modes of the oxides-supported species. These results provided a strong evidence for the clusters on the surface of oxides.

(v) In the ^{13}CO isotopic exchange reaction, the reactivity order was as follows: **1**/MgO ≪ **2**/SiO_2 ≪ **3**/SiO_2–Al_2O_3.

(vi) The reaction of **1**/MgO with CH_3I was very active at room temperature, whereas **2**/SiO_2 and **3**/SiO_2–Al_2O_3 were inactive at the same temperature. In contrast, the reaction of **3**/SiO_2–Al_2O_3 with CH_3Li was active, while **1**/MgO and **2**/SiO_2 were inactive at the same conditions.

(vii) Hydroformylation of ethylene proceeded with higher rates on the catalyst derived from **1**/MgO to give propanal and 1-propanol than on those from **2**/SiO_2 and **3**/SiO_2–Al_2O_3, but the rate for ethane production on the catalyst from **1**/MgO was lower.

The characterization and reactivities of various triruthenium ketenylidene clusters supported on oxides in CO isotopic exchange reactions, alkylation of CH_3I and CH_3Li, and ethylene hydroformylation are summarized in Table 5.

Acknowledgements

This work was supported by the National Natural Science Foundation of China, the Outstanding Foundation for Young Faculty in Education Committee of China, the Japan–US Cooperative Science Program, and the Foundation of Key Laboratory of Inorganic Hydrothermal Synthesis. We greatly thank Professor D.F. Shriver for his help in synthesizing some clusters.

References

[1] M. Ichikawa, Bull. Chem. Soc. Jpn. 51 (1978) 2273.
[2] M. Ichikawa, CHEMTECH 12 (1982) 674.
[3] Z. Xu, F.-S. Xiao, S.K. Purnell, O. Alexeev, S. Kawi, S.E. Deutsch and B.C. Gates, Nature 372 (1994) 346.
[4] B.C. Gates, L. Guczi and H. Konzinger (Eds.), Metal Cluster in Catalysis (Elsevier, Amsterdam, 1986).
[5] J.M. Basset, B.C. Gates, J.P. Candy, A. Choplin, M. Leconte, F. Quignard and C. Santini (Eds.), Surface Organometallic Chemistry: Molecular Approaches to Surface Catalysis (Kluwer Academic Publ., Dordrecht, 1988).
[6] Y.I. Yermakov, B.N. Kuznetsov and V.A. Zakharov (Eds.), Catalysis By Supported Complexes (Elsevier, Amsterdam, 1981).

[7] J.M. Basset and R. Ugo, in: Aspects of Homogeneous Catalysis, R. Ugo (Ed.) (Reidel, Dordrecht, 1977) p. 127.
[8] M. Ichikawa, Tailored Metal Catalysts, in: Iwasawa (Ed.) (Reidel, Dordrecht, 1986) p. 183.
[9] M.J. Sailor and D.F. Shriver, Organometallics 4 (1985) 1476.
[10] M.J. Sailor, C.P. Brock and D.F. Shriver, J. Am. Chem. Soc. 109 (1987) 6015.
[11] J. Hriljac and D.F. Shriver, J. Am. Chem. Soc. 109 (1987) 6010.
[12] M.J. Went, M.J. Sailor, P.L. Bogdan, C.P. Brock and D.F. Shriver, J. Am. Chem. Soc. 109 (1987) 6023.
[13] D.F. Shriver and M.J. Sailor, Acc. Chem. Res. 21 (1988) 374.
[14] A.J. Gordon and R.A. Ford, The Chemist's Companion (Wiley, New York, 1972).
[15] A.A. Davydov (Ed.), Infrared Spectroscopy of Adsorbed Species on the Surfaces of Transition Metal Oxides (Wiley, Chichester, 1990).
[16] M.L. Hair (Ed.), Infrared Spectroscopy in Surface Chemistry (Dekker, New York, 1982).
[17] L.H. Little (Ed.), Infrared Spectra of Adsorbed Species (Academic Press, New York, 1966).
[18] J.R. Sharpley, D.S. Strickland, G.M. George, M.R. Churchill and G. Bueno, Organometallics 2 (1983) 185.
[19] J.R. Andrews, D.B. Kettle, D.B. Powell and N. Sheppard, Inorg. Chem. 21 (1982) 2874.
[20] I.A. Oxton, Inorg. Chem. 21 (1982) 2877.
[21] J. Evans and G.S. McNulty, J. Chem. Soc. Dalton Trans. (1983) 639.
[22] V.D. Alexiev, N. Binsted, J. Evans, G.N. Greaves and R.J. Price, J. Chem. Soc. Chem. Commun. (1987) 395.
[23] H.P. Boehm and H. Knozinger, in: Catalysis (Science and Technology), R. Anderson and M. Boudart (Eds.)., Vol. 4 (New York, 1983).
[24] J.W. Ward, in: Zeolite Chemistry and Catalysis, J.A. Rabo (Ed.) (American Chemical Society, Washington, 1976).
[25] E.P. Parry, J. Catal. 2 (1963) 371.
[26] B.C. Gates, J. Mol. Catal. 86 (1994) 95.
[27] S.D. Maloney, F.B. van Zon, M.J. Kelley, D.C. Koningsberger and B.C. Gates, Catal. Lett. 5 (1990) 161.
[28] S. Kawi and B.C. Gates, Inorg. Chem. 31 (1992) 2939.
[29] S. Kawi, J.-R. Chang and B.C. Gates, J. Am. Chem. Soc. 115 (1993) 4830.
[30] J.R. Chang, Z. Xu, S.K. Purnell and B.C. Gates, J. Mol. Catal. 80 (1993) 49.
[31] H.H. Lamb, A.S. Fung, P.A. Tooley, J. Puga, T.R. Krause, M.J. Kelley and B.C. Gates, J. Am. Chem. Soc. 111 (1989) 8367.
[32] S.F.A. Kettle, Top. Current Chem. 71 (1977) 111.
[33] M. Deeba, B.J. Streusand, G.L. Schrade and B.C. Gates, J. Catal. 69 (1981) 218.
[34] A. Choplin, M. Leconte, J.M. Basset, S. Shore and W.L. Hsu, J. Mol. Catal. 21 (1983) 389.
[35] A. Theolier, A. Choplin, L. D'ornelas, J.M. Basset, C. Sourisseau, G.M. Zauderighi, R. Ugo and R. Psaro, Polyhedron 2 (1983) 119.
[36] P.S. Kirlin, F.A. DeThomas, W.J. Bailey, H.S. Gold, C. Dybowski and B.C. Gates, J. Phys. Chem. 90 (1986) 4882.
[37] M.J. Sailor, M.J. Went and D.F. Shriver, Inorg. Chem. 27 (1988) 2666.
[38] C.Q. Quicksall and T.G. Spiro, Inorg. Chem. 7 (1968) 2365.
[39] S. Pinchas and I. Laulicht (Eds.), Infrared Spectra of Labeled Compounds (Interscience, New York, 1972).
[40] F.A. Cotton and G. Wilkinson (Eds.), Advanced Inorganic Chemistry, 3rd Ed. (Interscience, New York, 1972).
[41] D.F. Shriver, P.W. Atkins and C.H. Langford, Inorganic Chemistry (Freeman, New York, 1989).
[42] F.-S. Xiao and M. Ichikawa, J. Catal. 147 (1994) 578.
[43] S.S.C. Chuang and S.I. Pien, J. Catal. 135 (1992) 618.